

Physicochemical Conditions of Formation of Gold and Silver Parageneses at the Valunistoe Deposit (Chukchi Peninsula)¹

T.V. Zhuravkova^{a,b,✉}, G.A. Palyanova^{a,b}, Yu.A. Kalinin^{a,b}, N.A. Goryachev^{c,d},
V.Yu. Zinina^{a,b}, L.M. Zhitova^{a,b}

^a Sobolev Institute of Geology and Mineralogy, Siberian Branch of the Russian Academy of Sciences,
pr. Akademika Koptyuga 3, Novosibirsk, 630090, Russia

^b Novosibirsk State University, ul. Pirogova 1, Novosibirsk, 630090, Russia

^c A.P. Vinogradov Institute of Geochemistry, Siberian Branch of the Russian Academy of Sciences,
ul. Favorskogo 1a, Irkutsk, 664033, Russia

^d N.A. Shilo Northeastern Complex Research Institute, Far Eastern Branch of the Russian Academy of Sciences,
ul. Portovaya 16, Magadan, 685000, Russia

Received 26 February 2019; received in revised form 15 May 2019; accepted 22 May 2019

Abstract—The mineral composition of ores from the Gornyi occurrence of the Valunistoe epithermal Au–Ag deposit (Chukchi Peninsula) has been studied. It has been found that, in addition to native gold, the Au–Ag mineralization comprises chalcogenides (uytenbogaardtite, petrovskaitite, acanthite, naumannite, and cervelleite) and minerals of the pearceite–polybasite series, which occur as microinclusions in fine-grained pyrite. The physicochemical conditions of formation of productive mineral assemblages have been estimated based on the chemical composition of Au and Ag minerals and their relationships with other minerals. It is shown that ores were deposited from weakly acid solutions at the late stages, on the background of a temperature decrease from 350 to 100 °C, a decrease in the fugacities of sulfur ($\log f_{S_2}$, from –2 to –23), tellurium ($\log f_{Te_2}$, from –5 to –27), and selenium ($\log f_{Se_2}$, from –16.5 to –28), and changes in the redox conditions ($\log f_{O_2}$, from –23 to –48).

Keywords: Au–Ag chalcogenides, Au–Ag solid solutions, physicochemical parameters of ore formation, Gornyi occurrence, Valunistoe deposit, Okhotsk–Chukchi volcanic belt

INTRODUCTION

The Valunistoe deposit is located in the Anadyr district of the Chukchi Autonomous Okrug (Fig. 1a). It is a typical epithermal Au–Ag deposit in the Okhotsk–Chukchi volcanic belt (OCVB). There are a few published data on the study of ore assemblages from the deposit (Volkov et al., 2006; Novoselov et al., 2010; Konstantinov, 2010; Korochkin, 2011). The leading scientists from TsNIGRI and IGEM RAS have distinguished two separate ore-forming events, which differ in vein mineralization, metasomatic alteration of host-rock, mineralogical and geochemical ore composition. Our investigation of the least studied Gornyi occurrence provided new information that was not previously reported. The occurrence is in the northeast flank of the deposit and is characterized by a number of specific features. The highest concentration of precious metals, Se and Te in

other areas of the Valunistoe deposit and specific mineralogical composition of ore assemblages attract our attention. This object is another example of deposits where Au–Ag chalcogenides (acanthite, uyttenbogaardtite, petrovskaitite, naumannite, pearceite, polybasite and others) are found in significant quantities.

The aim of this study is to investigate the features of the chemical composition of Au–Ag–S–Se–Te mineralization and the relationship between Au–Ag minerals and other minerals and to estimate the physicochemical conditions of their formation based on thermodynamic modeling. This study is a continuation of our series of articles on the study of the physicochemical parameters of the formation of Au–Ag deposits in the northeast of Russia (Rogovik, Kupol, Julietta, Junoe, Dorozhnoe, Ulakhan, Krutoe and others) (Savva and Pal'yanova, 2007; Pal'yanova and Savva, 2009; Savva et al., 2010, 2012, 2014; Pal'yanova et al., 2015; Palyanova et al., 2016; Kravtsova et al., 2017; Makshakov et al., 2017; Zhuravkova et al., 2017). Results of this study make a significant and fundamental contribution to understanding the genesis of this type of gold deposits and the development of their genetic models. Data on the diversity

¹This paper was translated by the authors.

✉ Corresponding author.

E-mail address: zhur0502@igm.nsc.ru (T.V. Zhuravkova)

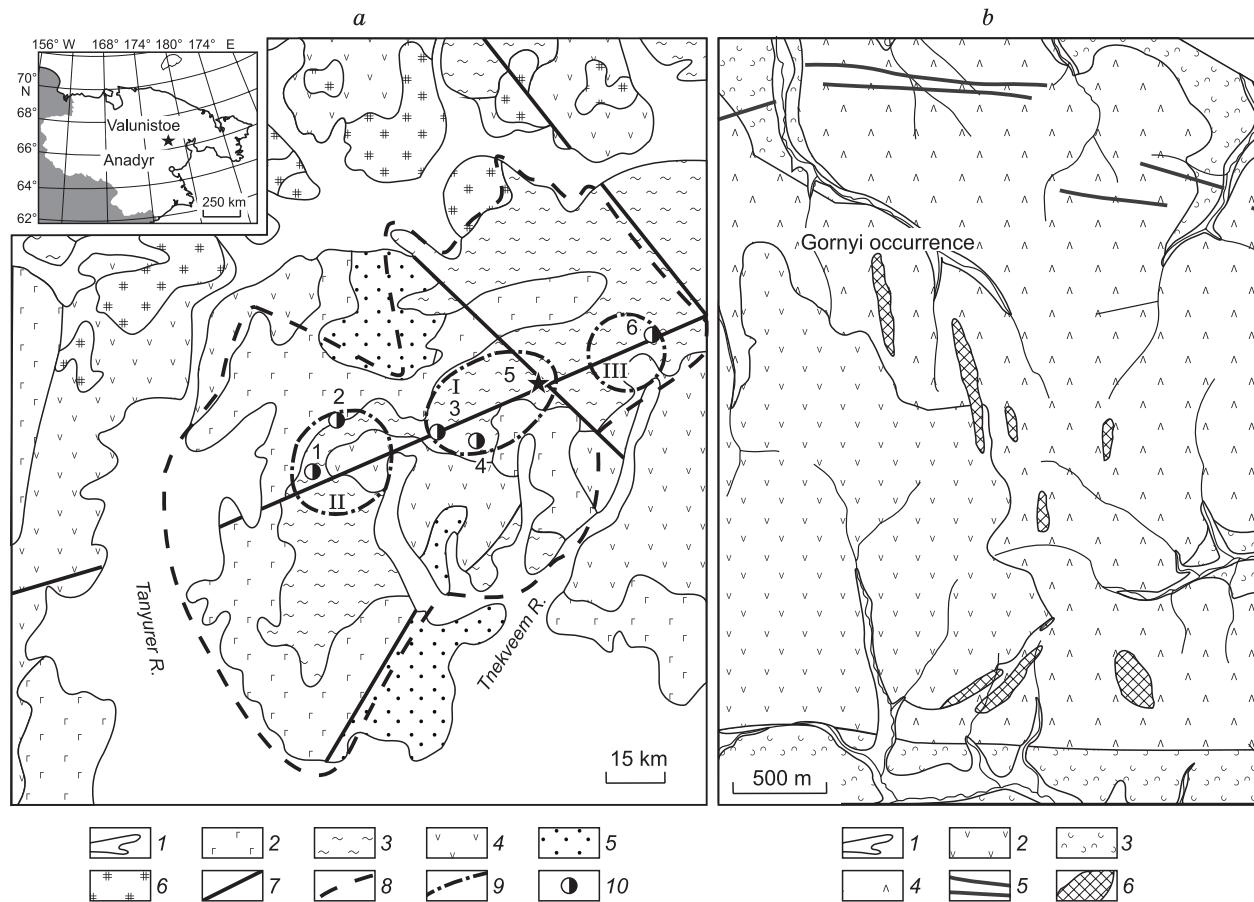


Fig. 1. Geological scheme of the Valunisty ore district (Konstantinov, 2010) with simplifications (*a*) and geological map of the Gornyi occurrence (Chitalin et al., 2016) (*b*). *a*: 1, Quaternary alluvial deposits; 2, Paleogene flood basalts, Upper Cretaceous–Paleogene basalts, andesites, rhyolites; 3, Upper Cretaceous rhyolites, rhyodacites, their tuffs and ignimbrites; 4, Upper Jurassic, Cretaceous andesites, dacites, rhyolites and their tuffs; 5, lower Carboniferous terrigenous deposits and Early Cretaceous granitoids; 6, Late Cretaceous granitoids; 7, faults; 8, borders of the ore field; 9, boundaries of ore district: I, Valunisty, II, Nygchekvaam, III, Terkenei; 10, gold-silver deposits/ore occurrences: 1, Osennii, 2, Nygchekvaam, 3, Zhil'nyi, 4, Shah, 5, Valunistoe, Gornyi, 6, Terkenei. *b*: 1, Quaternary alluvial deposits; 2, Upper Cretaceous andesites; 3, andesite tuffs; 4, Late Cretaceous subvolcanic rhyodacites; 5, faults; 6, vein-veinlet zones.

of Au–Ag minerals in ore assemblages are important information for the development of efficient technologies for processing ores and extracting precious metals from them.

GEOLOGICAL SETTING

The Valunistoe deposit is located within the Kanchalan–Amguem metallogenic zone (Volkov et al., 2006). Structurally, the field is located on the northern flank of the outer zone of the Okhotsk–Chukchi volcanic belt. The Valunistoe deposit belongs to two contiguous volcanic-dome structures—Valunistaya and Shalaya. The ore field is composed of the Upper Cretaceous volcanic rocks of intermediate and acid composition (Fig. 1*a*) (Korochkin, 2011).

The Gornyi occurrence is the northeastern flank of the Valunistoe deposit and includes two vein zones (the Tsentral'naya—submeridional strike and the Klyuchevaya—northeast). The zones are represented by steeply-dip-

ping quartz and quartz-adularia veins with weakly banded and breccia-like eruptive textures with fragments of andesites and dacites (Fig. 2). The width of zones is averages 10–15 m. Mineralized zones are hosted mainly by crystallitic-clastic tuffs of acidic and intermediate composition with superimposed hydrothermal mineralization (Fig. 1*b*). The host rocks are exposed to pre-ore propylitic (epidote–chlorite and chlorite–albite subzones) and syn-ore sericitic alteration. Sericitization is characteristic of the Valunistoe deposit and is one of the dominant alteration processes of primary volcanosedimentary rocks. It is worth noting that superficial hypergenic changes are manifested weakly.

Productive mineralization is represented by native gold and other minerals of Au and Ag, forming finely disseminated aggregates in quartz-adularia-sulfide veins and aggregates with signs of metacolloidal textures. The distribution of minerals of precious metals within the adularia-quartz veins is notably extremely uneven. Two productive mineral assemblages have been established: early gold-polysulfide

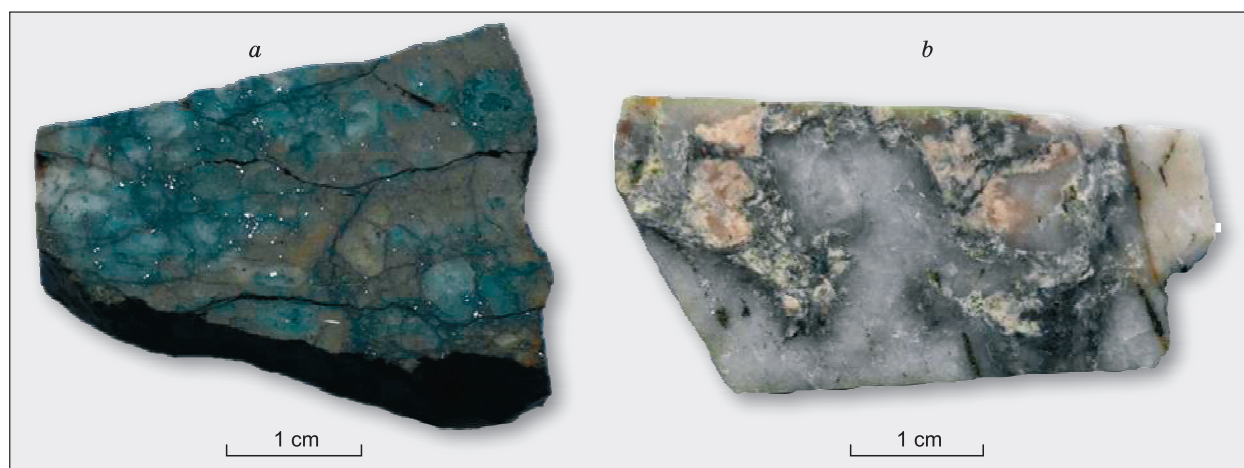


Fig. 2. Photographs of ore samples. *a*, Sample G-12, scattered sulfide impregnation in the altered host-rock; *b*, sample V-1, milky-white quartz with relics of altered host-rocks, along the boundaries of which sulfide mineralization is developed.

(with electrum and Pb, Zn, Cu sulfides) and late gold-sulfide-sulfosalts (with native gold of different fineness, Ag, Sb and Se-containing sulfosalts and chalcogenides). Formation of acanthite, uytenbogaardite, petrovskaita, naumannite, cervelleite, Au–Ag amalgams and minerals of the pearceite–polybasite series is related to the late stage of ore-forming processes.

MATERIALS AND METHODS

We have studied a collection of samples and their thin and polished sections. The samples were picked from technological sampling 2.5 t in weight from the exploration quarry of the Gornyi occurrence, which includes all the varieties of host rocks and ores. The specific features of chemical compositions and relationships of gold and silver minerals were analyzed using optical and scanning microscopy and microprobe analysis (Analytical Center for Multi-Elemental and Isotope Research SB RAS, Russia, Novosibirsk, analyst N.S. Karmanov).

The $\log f_{S_2}$ – $\log f_{Se_2}$, $\log f_{S_2}$ – $\log f_{Te_2}$, $\log f_{S_2}$ – $\log f_{O_2}$ diagrams were constructed for temperatures 25–350 °C by the procedure of Garrels and Christ (1968). Gibbs free energies (G_T) used in the calculations of equations of reactions with participation of minerals Fe, Cu, Zn and Pb were borrowed from the database of the “Selector-Windows” software (Chudnenko, 2010): *s_sprons07.DB* for sulfides and oxides (Helgeson et al., 1978) and *s_Yokokawa.DB* for selenides and tellurides (Yokokawa, 1988). In the calculations of G_T of Au–Ag minerals we used thermodynamic data from original sources (Tagirov et al., 2006; Pal’yanova, 2008; Echmaeva and Osadchii, 2009; Pal’yanova et al., 2014; Voronin, 2017). Reactions with participation of cervelleite were calculated using the method from (Simon and Essene, 1996).

GOLD MINERALIZATION FEATURES

Peculiarities of the mineral composition indicate that the gold-silver Valunistoe deposit is a typical epithermal object of the Okhotsk–Chukchi volcanic belt, related to the Upper Cretaceous volcanic rocks of the “ore-bearing andesite–ignimbrite–granodiorite association” (Konstantinov, 2010). The ore bodies are characterized by rhythmically banded textures, the dark bands of which contain fine-grained Au–Ag minerals. The granulometric composition of the concentrate of technological sample is presented in Table 1.

The percentage of sulfides of iron, copper, lead and zinc in the ores from the Gornyi occurrence is commonly 1–2%, which is nearly 2 times lower than at the Valunistoe deposit on the whole. The grain sizes of ore minerals are no more than 1–3 mm. Data of operational exploration show that the concentrations of Au and Ag in the ores average 13.4 ppm and 101.9 ppm, respectively. Ore minerals are dominated by pyrite, and they also contain sphalerite, chalcopyrite, galena, native gold, Au–Ag sulfides (acanthite, uytenbogaardite, petrovskaita), cervelleite and minerals of pearceite–polybasite series.

Pyrite occurs as single impregnations of both xenomorphic and idiomorphic grains—cubic, pentagon-dodecahedral, less frequently, octahedral crystals containing microinclusions of ore minerals, or forms fine-grained porous aggregates. Pyrite is intergrown with chalcopyrite, sphalerite and native gold. Pyrite contained inclusions of greenockite (CdS), in which minor amounts of Zn and Fe (2.1 and 2.3 wt.%, respectively) were present.

Chalcopyrite, galena, and sphalerite form impregnations of xenomorphic grains in quartz and are frequently intergrown with pyrite or occur as inclusions in the outer zones of pyrite. Chalcopyrite, occasionally with sphalerite, occurs as inclusions in native gold. In later associations, chalcopyrite is replaced by covellite, and galena, by angle-

Table 1. Granulometric composition of the concentrate of technological samples from the open pit of Gornyi occurrence

Size of fraction, mm	Content in concentrate, %	Minerals, %
>0.25	10	Intergrowths of pyrite and quartz—20 Fragments of galena crystals—10 Pyrite crystals and their fragments—70
0.16–0.25	15–20	Pyrite crystals—70 Fragments of galena crystals—15 Intergrowths of pyrite and quartz—10 Garnet—1–3 Epidote—1–2 Sphene, leucoxene—signs
Magnetic	1–2	Spheres of magnetite—1–2 Magnetite crystals—50 Fragments of metal shavings—50
<0.16	70–75	Pyrite crystals and their fragments—80 Fragments of galena crystals—18–20 Non ore—1–2
Tailings of bromoform (from fraction <0.16)	95	Pyrite crystals—80 Fragments of galena crystals—20 Garnet, sphene, leucoxene, epidote—signs
Heavy concentrate (from fraction <0.16)	5	Native gold—50–70 signs (5–7) Acanthite—2–3 Pyrite—70–75 Galena—20–25

site (PbSO₄). Sphalerite contains minor impurities of Fe (to 2 wt.%) and Cd (0.8–8.75 wt.%).

The minerals of Au and Ag are represented by native gold of varying fineness² (from high-fineness gold to electrum up to native silver) as well as by amalgams, acanthite (Ag₂S), uytenbogaardtite (Ag₃AuS₂), petrovskaitite (AgAuS), naumannite (Ag₂Se), cervelleite (Ag₄STe) and minerals of pearceite–polybasite series ((Ag,Cu)₁₆(Sb,As)₂S₁₁).

Electrum (450–640‰) is localized in pyrite (Fig. 3a) and forms intergrowths with sphalerite, acanthite and uytenbogaardtite in quartz. Electrum grains have nonuniform composition (Table 2, Fig. 3b). Ag-rich electrum (310–370‰) together with its Hg variety (Hg to 6.9 wt.%) forms intergrowths (Fig. 3b) or veinlets in electrum (570–640‰). High-fineness gold (750–950‰) occurs mainly as rims and veinlets in electrum. In addition, there are also single grains of fineness 840–850‰, the marginal parts of which are depleted in silver (950–990‰). Native silver contains inclusions of minerals of pearceite–polybasite series and is replaced by acanthite (Fig. 3c).

Hg-rich silver together with Ag-rich electrum is intergrown with the minerals of pearceite–polybasite series and is characterized by wide variations in composition (Table 2).

Au–Ag sulfides form rims and veinlets in electrum (Fig. 4a, b), and their composition is characterized by an excess of S and wide variations in Au and Ag (Table 3). The

mineral phase, similar in composition to uytenbogaardtite, was found to contain minor Se (to 3.62 wt.%). These phases do not always correspond to the stoichiometry of uytenbogaardtite and petrovskaitite, which suggests either the presence of phase mixtures (Ag₂S + Ag₃AuS₂, AgAuS + Ag₃AuS₂), or the existence of solid solutions Ag_{2-x}Au_xS (Pal'yanova et al., 2011; Tauson et al., 2018).

Acanthite-I with electrum (Fig. 3d) or galena form inclusions in pyrite and intergrowths with naumannite and chalcopyrite (Fig. 4c). Acanthite-I contains from 1.6 to 8.4 wt.% Se, and naumannite, to 2.1 wt.% S (Table 3). Acanthite-II with uytenbogaardtite and copper sulfides occurs as rims and veins in other minerals and contains to 3.3 wt.% Se.

Cervelleite (to 0.8 wt.% Se) and galena form microinclusions in pyrite (Fig. 4d). The contents of sulfur and tellurium in cervelleite are higher than stoichiometric (Table 3).

Minerals of pearceite–polybasite series ((Ag,Cu)₁₆(Sb,As)₂S₁₁) occur mainly in the intergrowths with electrum, native silver and Au–Ag amalgams. A specific feature of the minerals of this series, occurring in association with native silver, is their fracturing. It is most likely related to the change in the volume of mineral phases during crystallization. They contain Fe (to 1.3 wt.%), Se (0.7–1.9 wt.%) and Te (to 5.8 wt.%). Earlier, the ores from the Valunistoe deposit were found to contain Se-bearing arsenopolybasite (to 5.1 wt.% Se), mineral of pearceite–polybasite series, in which antimony was absent (Novoselov et al., 2010).

Mineralogical investigations of the ores showed that their formation proceeded in two stages. Originally, sulfides of Fe, Zn, Cu together with native gold, and later the Se-bearing mineralization were formed. It was revealed that naumannite formed prior to Se-acanthite, and the replacement of chalcopyrite by covellite took place at the last stage of mineral formation. The development of acanthite, uytenbogaardtite and petrovskaitite after native gold indicates the high potential of sulfur during the formation of precious metal mineralization.

PHYSICO-CHEMICAL PARAMETERS OF ORE FORMATION (THERMODYNAMIC MODELING)

The presence of Fe-sphalerite, Se-acanthite, S-naumannite, cervelleite, native gold of various finenesses, Au–Ag sulfides and other minerals in the mineral assemblages allowed the estimation of the following physicochemical parameters of ore-forming processes: T , f_{S_2} , f_{Se_2} and f_{Te_2} . Earlier, on the example of the Rogovik deposit (northeastern Russia) we showed the possibility of using the compositions of Se-acanthite and S-naumannite for the estimation of both the temperature and fugacity of S and Se (Zhuravkova et al., 2015). Sulfur fugacity (f_{S_2}) and temperatures of mineral formation were estimated using the electrum-sphalerite geothermometer. This geothermometer is widely used by various authors (Scott and Barnes, 1971; Barton and Skinner, 1979; Moloshag, 2009; Lyubimtseva et al., 2018) and is

² We adhere to the terminology used in (Boyle, 1979): “high-fineness gold” (1000–700‰), “electrum” (250–700‰), “kustelite” (100–250‰) and “native silver” (0–100‰).

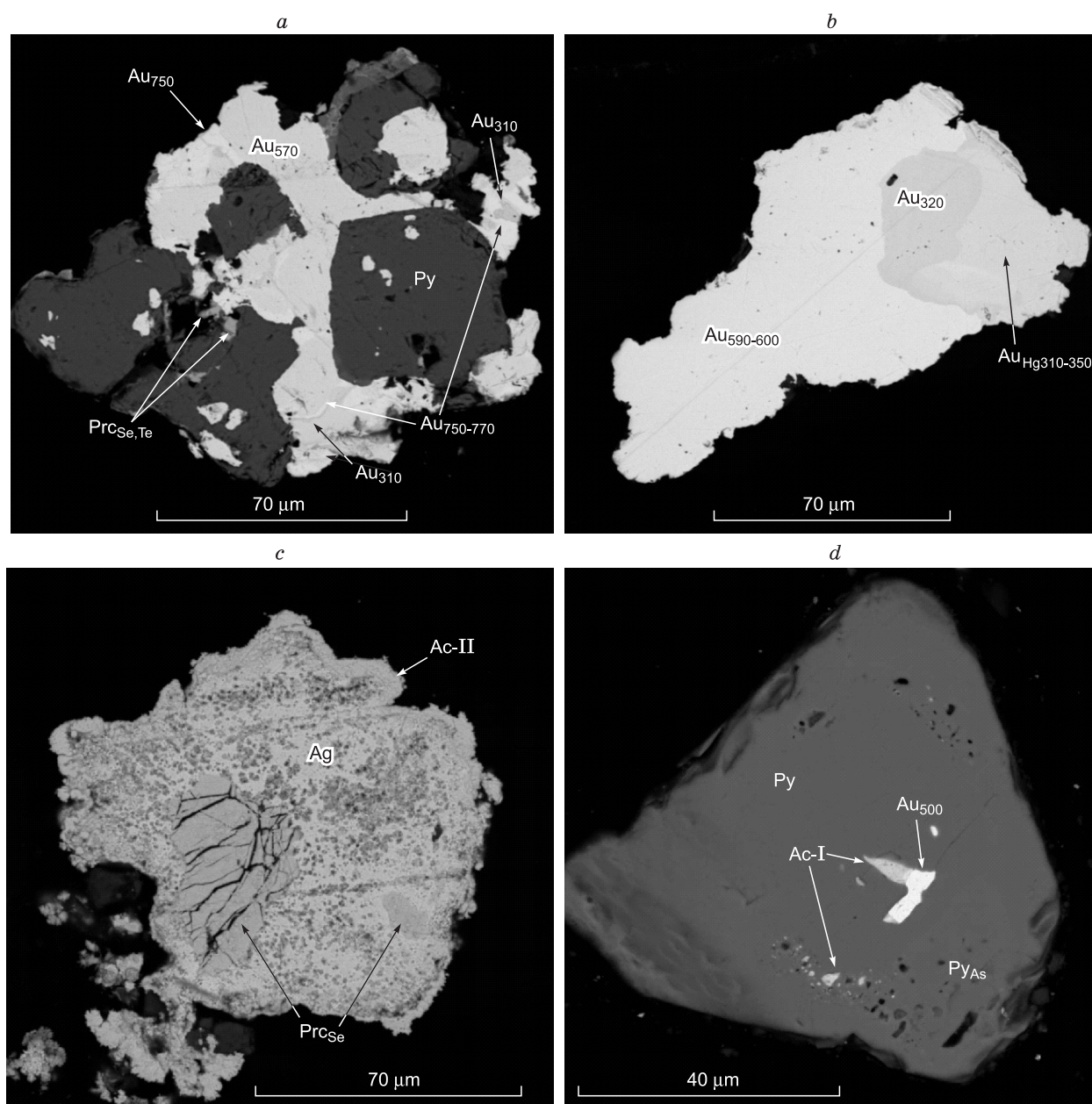


Fig. 3. SEM photomicrographs of ore minerals. *a*, Assemblage of pyrite (Py), pierceite-polybasite (Prs) and electrum with high-finesness gold veinlets; *b*, intergrown electrum and Au–Ag amalgam; *c*, native silver with inclusions of pierceite-polybasite and rims of acanthite; *d*, microinclusion of electrum (Au_{500}) and acanthite (Ac-I) in zonal pyrite.

based on the data on the Fe content of sphalerite (X_{FeS}) and amount of Ag ($X_{Ag} = Ag/(Ag + Au)$) in coexisting native gold. To calculate the temperature and fugacity values of S, we borrowed equations from (Scott and Barnes, 1971) and (Barton and Skinner, 1979).

In this paper we have studied homogeneous grains of native gold in paragenesis with sphalerite. The composition of native gold from this paragenesis is close to $X_{Ag} = 0.34$, and Fe content of sphalerite (with low concentrations of Cd) $X_{FeS} = 0.02$. The calculations showed that the formation of this paragenesis with the specified contents of native gold

and sphalerite requires temperatures of 350–360 °C and sulfur fugacity $\log f_{S_2} = -6.75 \dots -6.98$. Calculated by different equations, these characteristics have similar values.

In addition, results of mineralogical studies of the deposit were used for thermodynamic calculations and construction of the diagram $\log f_{S_2} - \log(f_{Se_2}, f_{Te_2}, f_{O_2})$ in the temperature range of 100–350 °C for mineral equilibria with participation of electrum of composition $Ag_{0.75}Au_{0.25}$ (380%) and $Ag_{0.5}Au_{0.5}$ (650%), as well as sulfides, selenides, and tellurides Ag, Au, Cu, Fe and Pb (Fig. 5*a, b*). The limit values of fugacity of S, Se and Te were determined

Table 2. Chemical composition of native gold, silver and Au–Ag amalgams

Element content, wt. %						N _{Au} , ‰	Mineral associations
Ag	Au	Hg	Cu	S	Total		
Au-rich electrum							
46.83	54.36	–	–	–	101.19	537	Ac-I ± Py in Q
54.48	45.16	–	–	–	99.64	453	Ac-I ± Py in Q
48.12	51.81	–	–	–	99.93	518	With Uyt rim
40.75	60.43	–	–	–	101.18	597	Au ₃₂₀ and Au _{Hg310–350}
35.93	63.40	–	–	–	99.33	640	Au ₃₂₀ and Au _{Hg310–350}
Ag-rich electrum							
68.44	30.63	–	–	–	99.06	310	Au _{590–640} + Au _{Hg310–350}
55.39	42.77	–	–	–	98.15	436	Au _{590–640} + Au _{Hg310–350}
63.48	35.57	–	0.61	2.60	102.26	359	Ag _{Hg} + Kust _{Hg} + Prc
Hg-rich electrum (El _{Hg})							
61.90	30.97	6.87	–	–	99.75	310	Au _{590–600} + Au ₃₂₀
59.12	35.06	5.61	–	–	99.79	351	Au _{590–600} + Au ₃₂₀
60.43	35.15	6.00	–	–	101.58	346	(Au _{610–640} + Au _{310–440} + Au _{Hg350–380}) with inclusions of Ccp + Sp and rim of Ac-II + Uyt
High-fineness gold (Au)							
16.03	84.42	–	–	–	100.45	840	Heterogeneous grain
0.72	97.43	–	–	–	98.14	993	Heterogeneous grain
25.01	73.97	–	–	–	98.98	747	Au _{500–600} + Py + Prc
27.43	71.27	–	–	–	98.7	722	In Au _{610–630}
Hg-rich kustelite (Kust _{Hg})							
73.03	18.27	8.06	–	1.31	100.67	184	Au ₃₆₀ + Ag _{Hg} + Prc
Native silver (Ag)							
97.71	–	–	0.41	1.32	99.44	0	With inclusions of Prc and rim of Ac-II
Hg-rich silver (Ag _{Hg})							
84.30	8.21	9.15	–	–	101.66	81	El ₃₆₀ + Kust _{Hg} + Prc
88.35	3.14	7.41	–	0.55	99.45	32	El ₃₆₀ + Kust _{Hg} + Prc

Note. Here and in Table 3: N_{Au}, gold fineness; Q, quartz; Py, pyrite; Ccp, chalcopyrite; Sp_{Cd}, Cd-containing sphalerite; Ga, galena; Ac, acanthite; Nmt, naumannite; Cerv, cervelleite; Kust, kustelite; Uyt, uytenbogaardite; Pet, petrovskaite; Prc, minerals of pearceite–polybasite series.

from the stability lines of minerals of the main productive associations.

The presence of electrum in association with pyrite, sphalerite and chalcopyrite allows estimation of $\log f_{S_2}$ values. At 350 °C, these minerals are stable at $\log f_{S_2} = -10 \dots -5$ and $\log f_{O_2} < -24$ (Fig. 5a, b). The obtained values of sulfur fugacity correlate with the estimated values calculated using the electrum-sphalerite geothermometer.

Cervelleite (Ag₄STe) together with galena occurs as inclusions in pyrite. The stability field of Ag sulfotelluride at 350 °C is limited by the interval $\log f_{Te_2} = -15 \dots -5$, and at 100 °C, $\log f_{Te_2} = -27 \dots -14$ (Fig. 5a). The stability line of pyrite-pyrrhotite (FeS₂/FeS) at 350 °C sets minimum values $\log f_{S_2} > -10$ and maximum values $\log f_{O_2} < -20$, and at 100 °C, $\log f_{S_2} = -25$ and $\log f_{O_2} < -39$ (Fig. 5a, b).

The phases of solid solution of naumannite series (Ag_{2.18}S_{0.19}Se_{0.81}) are closely intergrown with pyrite and chalcopyrite. The formation of this association at 100 °C is

limited by the stability lines of chalcopyrite ($\log f_{S_2} < -17.5$, $\log f_{O_2} < -49$) and solid solution of naumannite series of the specified composition ($\log f_{S_2} > -23$, $\log f_{Se_2} = -27 \dots -21.5$, $\log f_{Te_2} < -25$) (Fig. 5c, d). The presence of Se-acanthite-I (Ag_{1.65}S_{0.96}Se_{0.04} – Ag_{2.06}S_{0.72}Se_{0.28}) together with galena, pyrite, chalcopyrite in the mineral assemblages under study allows one to distinguish their stability field. The composition of the mineral association indicates that the limit values of S fugacity correspond to the stability lines of Se-acanthite and chalcopyrite ($\log f_{S_2} = -22 \dots -17.5$), and Se fugacity is restricted only by the stability lines of Se-acanthite ($\log f_{Se_2} = -28 \dots -23.5$) (Fig. 5c, d).

The rims of acanthite-II and Au–Ag sulfides on electrum are the latest to form. At 100 °C, $\log f_{S_2} \geq -16$ values correspond to the lower boundary of the appearance of uytenbogaardite during the sulfidization of electrum (Ag_{0.75}Au_{0.25}). The presence of acanthite-II (Ag₂S–Ag_{1.77}S_{0.91}Se_{0.09}) in association with Au–Ag and Cu sulfides allows estimation of

the maximum values of $\log f_{\text{Se}_2}$ (<-16.5) and $\log f_{\text{O}_2} <-48$ (Fig. 5c, d) at which this mineral association forms.

Hydrothermal alterations of ore-hosting rocks from the Gornyi occurrence are represented by the processes of metasomatic replacement of rocks: pre-ore propylitization and syn-ore sericitization. According to Zharikov and Rusinov (1998), pH of ore-forming solutions varies from 2 to 5, depending on the type of metasomatic alterations of the host rocks.

DISCUSSION

Au–Ag chalcogenides frequently occur in the mineral assemblages of epithermal deposits (Warmada et al., 2003;

Plotinskaya et al., 2009; Savva et al., 2012; Palyanova et al., 2014). Their origin is related to the increased fugacity of S, Se and (or) Te. Unlike the Valunistoe deposit discussed above, the Bereznyakovskoe deposit (Ural, Russia) contains abundant Au–Ag tellurides (sylvanite, krennerite, calaverite, petzite, hessite and stützite) in association with fahlores (Plotinskaya et al., 2009), and native gold is rare and occurs in later associations. Telluride association at this object formed in the temperature range of 220–185 °C and pressures of 0.4–0.2 kbar with the leading role of Te in the ore-forming process. The presence of Ag sulfotelluride (cervelleite) and the absence of Au–Ag tellurides in the studied mineralogical assemblages of the Valunistoe deposit suggest

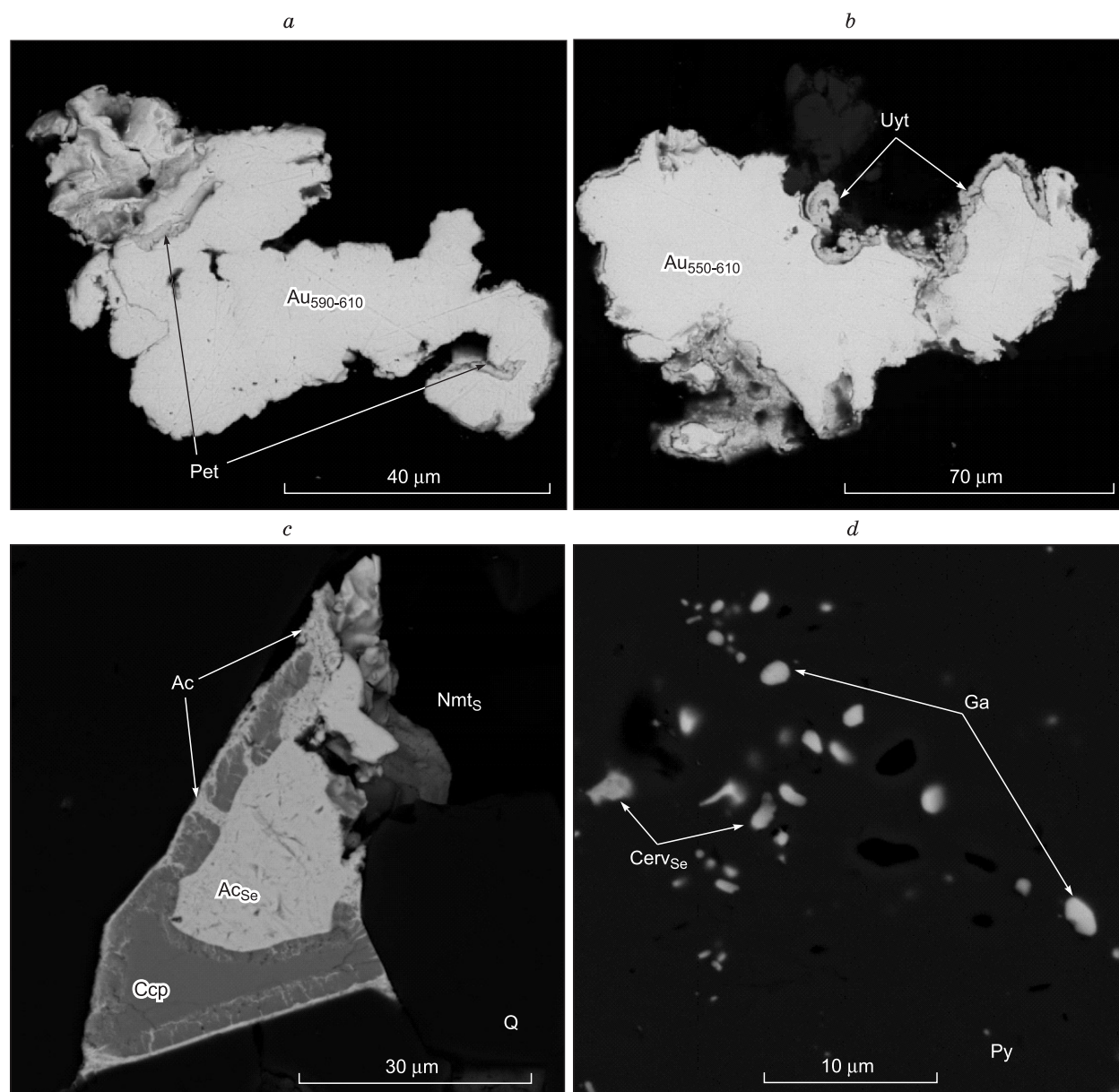


Fig. 4. Mineral assemblages of gold and silver chalcogenides (SEM photomicrographs). *a, b*, Petrovskaitite (Pet) and uyenbogaardtite (Uyt) rims on electrum (550–610%); *c*, rims of acanthite on chalcopyrite and Ag-sulfoselenides; *d*, microinclusions of Se-cervelleite (Cerv_{se}) and galena (Ga) in pyrite (Py).

Table 3. Chemical composition of gold and silver chalcogenides

Element content, wt. %						Formula	Mineral associations
Au	Ag	S	Se	Te	Total		
S-naumannite (Nmt_S)							
–	75.18	1.95	20.39	–	97.52	Ag _{2.18} S _{0.19} Se _{0.81}	In Ac-I
–	78.04	2.06	21.72	–	101.82	Ag _{2.13} S _{0.19} Se _{0.81}	With rim of Ac-II in Q
Se-acanthite (Ac-I)							
–	80.12	13.16	4.97	–	98.25	Ag _{1.57} S _{0.87} Se _{0.14}	In Py
–	84.11	13.53	2.36	–	100.00	Ag _{1.73} S _{0.93} Se _{0.07}	In Py
–	84.55	8.76	8.43	–	101.74	Ag _{2.06} S _{0.72} Se _{0.28}	Py + Ga in Ccp
–	85.13	12.09	2.73	–	99.95	Ag _{1.92} S _{0.92} Se _{0.08}	Py in Q
–	83.00	14.29	1.64	–	98.93	Ag _{1.65} S _{0.96} Se _{0.04}	With inclusions of Ga
–	81.24	9.99	7.12	–	98.35	Ag _{1.87} S _{0.78} Se _{0.22}	With inclusion of Au _{564–580}
–	85.40	12.78	2.40	–	100.58	Ag _{1.85} S _{0.93} Se _{0.07}	Ccp + Nmt, with rim of Ac-II, in Q
Acanthite (Ac-II)							
–	89.23	9.09	–	–	98.32	Ag _{1.97} S	Rim on Ga
–	86.62	13.07	–	–	99.69	Ag _{1.97} S	Py + Ac-I
–	85.06	11.79	1.48	–	98.33	Ag _{2.04} S _{0.95} Se _{0.05}	In Q
–	84.09	12.86	2.92	–	99.87	Ag _{1.78} S _{0.92} Se _{0.08}	Ccp
–	85.34	13.00	3.28	–	101.62	Ag _{1.77} S _{0.91} Se _{0.09}	Ccp
Cervelleite (Cerv)							
–	61.09	6.40	0.79	31.15	99.43	Ag _{3.33} S _{1.17} Se _{0.06} Te _{1.44}	In Py
Uytenbogaardite (Uyt)							
33.31	53.28	11.94	–	–	98.53	Ag _{2.86} Au _{0.98} S _{2.16}	Rim on Au _{510–606}
40.00	45.58	12.02	–	–	97.60	Ag _{2.53} Au _{1.22} S _{2.25}	Rim on Au _{520–540}
34.17	53.66	9.87	3.62	–	101.32	Ag _{2.91} Au _{1.02} S _{1.80} Se _{0.27}	Rim on Au _{520–540}
38.14	49.51	10.87	1.85	–	100.37	Ag _{2.71} Au _{1.14} S _{2.0} Se _{0.14}	Rim on Au _{520–540}
Petrovskaita (Pet)							
44.09	34.07	10.99	–	–	89.15	Ag _{1.07} Au _{0.76} S _{1.47}	Rims and veinlets in Au _{590–606}
46.55	39.32	11.11	–	–	96.97	Ag _{1.15} Au _{0.75} S _{1.10}	Rims and veinlets in Au _{590–606}

that, during ore deposition, the fugacities of Te had lower values of f_{Te_2} compared to the Bereznyakovskoe deposit.

Au–Ag sulfides (acanthite, uytenbogaardite, petrovskaita) and selenides (naumannite, fischerite) together with native gold are widely spread at the Kupol deposit, which is one of the largest gold-silver deposits in Chukchi Peninsula (Savva et al., 2012). The presence of intergrowths of Au–Ag sulfides and selenides suggest that they were formed at the same time, and the increased selenium content of minerals (to 5.6 wt.% in uytenbogaardite, to 14.5 wt.% in acanthite, from 2.3 to 3.1 wt.% in pyrargyrite, and to 4. wt.% in polybasite) indicates the high fugacities of both S and Se in ore-forming processes. The mineral assemblages from the Gornyi occurrence have similar characteristics with Au–Ag mineralization of the Kupol deposit but differ in the absence of complex Au–Ag selenides. At the Kupol deposit, Au–Ag sulfides and selenides are associated with native sulfur and jarosite, which suggests oxidized environments of mineral formation and participation of more acidic solutions com-

pared to the studied mineral assemblages from the Gornyi occurrence.

One more analog of the Valunistoe deposit is the epithermal Pongkor deposit (Indonesia) (Warmada et al., 2003), which also has similar ore formation conditions and parageneses of native gold with Au–Ag sulfides, selenides, and sulfosalts.

CONCLUSIONS

Thus, our investigations show that the formation of Au–Ag chalcogenides took place at the late stages of ore-forming process from weakly acid solutions on the background of a decrease in temperature from 350 to 100 °C and in the fugacities of sulfur ($\log f_{S_2}$ from -2 to -23), tellurium ($\log f_{Te_2}$ from -5 to -27) and selenium ($\log f_{Se_2}$ from -16.5 to -28), and change in the redox conditions of mineral formation ($\log f_{O_2}$ from < -23 to $\log f_{O_2} < -48$).

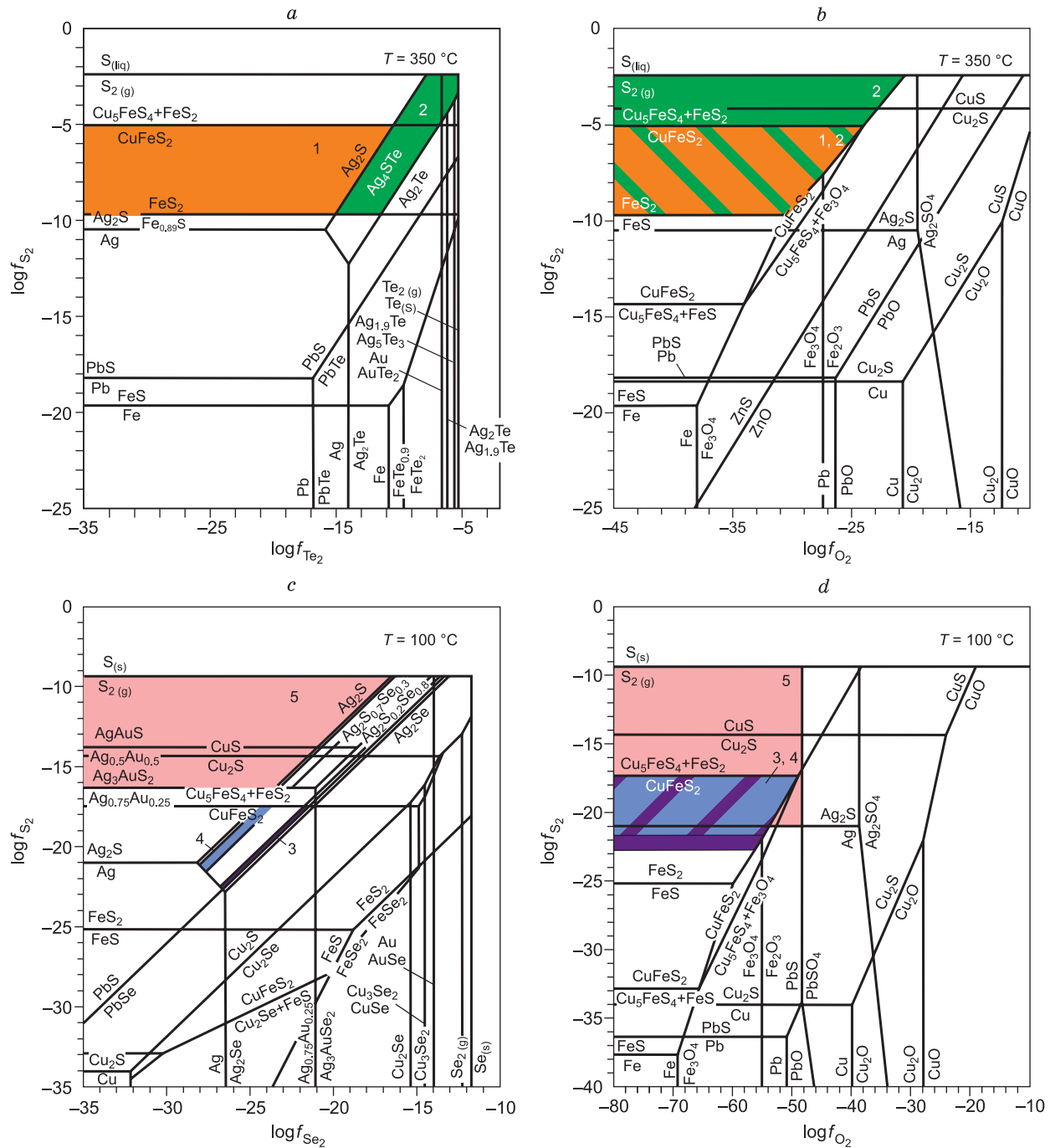


Fig. 5. $\log f_{S_2}$ – $\log f_{Te_2}$ and $\log f_{S_2}$ – $\log f_{O_2}$ diagrams at 350 °C (a, b) and $\log f_{S_2}$ – $\log f_{Se_2}$ and $\log f_{S_2}$ – $\log f_{O_2}$ diagrams at 100 °C (c, d) and fields of stability of minerals and their associations. 1, electrum + pyrite + sphalerite + chalcopyrite; 2, cervelleite + galena + pyrite; 3, silver sulfoselenide of the naumannite series ($Ag_2Se_{0.8}S_{0.2}$) + sphalerite + pyrite; 4, silver sulfoselenides of acanthite series ($Ag_2S_{0.9}Se_{0.1}$ – $Ag_2S_{0.7}Se_{0.3}$) + galena + pyrite + chalcopyrite; 5, Au–Ag and Cu-sulfides.

A specific feature of the studied flank of the Valunistoe deposit is that Au and Ag chalcogenides (uytenbogaardite, petrovskaita, acanthite, naumannite, cervelleite) and minerals of pearceite–polybasite series are present in the same quantities as native gold. Their presence in the form of microinclusions in pyrite makes it difficult to use traditional schemes for the enrichment and extraction of precious met-

als. The obtained data on the specific features of compositions of Au and Ag minerals and their relationships with other minerals are important for the development of rational schemes of extraction of Au and Ag from refractory ores.

We are thankful to V.V. Lebedev, A.S. Vas'kov and V.P. Bondarenko for the provided materials, and to Dr N.S. Karmanov (IGM SB RAS) for the microprobe analysis

of mineral compositions. The work was done on state assignment of IGM SB RAS and ICCT SB RAS financed by the Ministry of Science and Higher Education of the Russian Federation.

REFERENCES

- Barton, P.B. Jr., Skinner, B.J., 1979. Sulfide mineral stabilities, in: Barnes, H.L. (Ed.), *Geochemistry of Hydrothermal Ore Deposits*. John Wiley and Sons, New York, pp. 278–403.
- Chitalin, A.F., Agapitov, D.D., Shtengelov, A.R., Usenko, V.V., Fomichev, E.V., Grishin, E.M., Voskresenskii, K.I., 2016. Shear tectonics and gold-bearing capacity of the Kolyma–Chukchi Peninsula region, in: *Minex Far East Conf. (Magadan, 14–15 July 2016)* [in Russian] https://minexforum.com/wp-content/uploads/2016/07/4.Chitalin-i-dr_Sdvigovaya-tektonika-i-zolotonosnost-Kolymsko-Chukotskogo-regiona_2016.pdf.
- Chudnenko, K.V., 2010. *Thermodynamic Modeling in Geochemistry: Theory, Algorithms, Software, Applications* [in Russian]. Geo, Novosibirsk.
- Echmaeva, E.A., Osadchii, E.G., 2009. Determination of the thermodynamic properties of compounds in the Ag–Au–Se and Ag–Au–Te systems by the EMF method. *Geol. Ore Deposits* 51 (3), 247–258.
- Garrels, R.M., Christ, C.L., 1965. *Solution, Minerals, and Equilibria*. Harper and Row, New York.
- Helgeson, H.C., Delany, J.M., Nesbitt, H.W., Bird, D.K., 1978. Summary and critique of the thermodynamic properties of rock-forming minerals. *Am. J. Sci.* 278-A, 1–229.
- Konstantinov, M.M., 2010. *Gold Deposits of Russia* [in Russian]. Akvarel', Moscow.
- Korochkin, E.N., 2011. Assessment of the prospects of the Konchalan–Amgum license area in the Gornyi and Ognennyi sites, in: *Xth Int. Conf. “New Ideas in Earth Sciences” (12–15 April 2011)*, Reports, Vol. 1 [in Russian]. Extra-Print, Moscow, p. 208.
- Kravtsova, R.G., Tauson, V.L., Palyanova, G.A., Makshakov, A.S., Pavlova, L.A., 2017. Specific composition of native silver from the Rogovik Au–Ag deposit, Northeastern Russia. *Geol. Ore Deposits* 59 (5), 375–390.
- Lyubimtseva, N.G., Bortnikov, N.S., Borisovsky, S.E., Prokofiev, V. Yu., Vikent'eva, O.V., 2018. Fahlore and sphalerite from the Darasun gold deposit in the Eastern Transbaikalian region, Russia: II. Fe and Zn partitioning, fluid inclusions, and formation conditions. *Geol. Ore Deposits* 60 (3), 220–240.
- Makshakov, A.S., Kravtsova, R.G., Goryachev, N.A., Pal'yanova, G.A., Pavlova, L.A., 2017. First discovery of high-mercury silver in ores of the Rogovik gold–silver deposit (Northeastern Russia). *Dokl. Earth Sci.* 476 (1), 1094–1098.
- Moloshag, V.P., 2009. Application of mineral composition for assessment of physical-chemical conditions of massive sulfide ores formation in the Urals. *Litosfera*, No. 2, 28–40.
- Novoselov, K.A., Kotlyarov, V.A., Belogub, E.V., 2010. Silver sulfoselenide from ore of the Valunisty Au–Ag deposit, Chukchi Peninsula. *Geol. Ore Deposits* 52 (8), 811–814.
- Pal'yanova, C.A., 2008. *Physicochemical Characteristics of the Behavior of Gold and Silver in the Processes of Hydrothermal Ore Formation* [in Russian]. Izd. SO RAN, Novosibirsk.
- Pal'yanova, G.A., Savva, N.E., 2009. Specific genesis of gold and silver sulfides at the Yunoe deposit (Magadan Region, Russia). *Russian Geology and Geophysics (Geologiya i Geofizika)* 50 (7), 587–602 (759–777).
- Pal'yanova, G.A., Kokh, K.A., Seryotkin, Yu.V., 2011. Formation of gold and silver sulfides in the system Ag–Au–S. *Russian Geology and Geophysics (Geologiya i Geofizika)* 52 (4), 443–449 (568–576).
- Pal'yanova, G.A., Chudnenko, K.V., Zhuravkova, T.V., 2014. Thermodynamic properties of solid solutions in the system Ag_2S – Ag_2Se . *Thermochim. Acta* 575, 90–96.
- Pal'yanova, G.A., Kravtsova, R.G., Zhuravkova, T.V., 2015. $Ag_2(S,Se)$ solid solutions in the ores of the Rogovik gold–silver deposit (northeastern Russia). *Russian Geology and Geophysics (Geologiya i Geofizika)* 56 (12) 1738–1748 (2198–2211).
- Palyanova, G., Karmanov, N., Savva, N., 2014. Sulfidation of native gold. *Am. Mineral.* 99 (5–6), 1095–1103.
- Palyanova, G.A., Savva, N.E., Zhuravkova, T.V., Kolova, E.E., 2016. Gold and silver minerals in low-sulfidation ores of the Julietta deposit (northeastern Russia). *Russian Geology and Geophysics (Geologiya i Geofizika)* 57 (8), 1171–1190 (1488–1510).
- Plotinskaya, O.Yu., Groznova, E.O., Kovalenker, V.A., Novoselov, K.A., Seltmann, R., 2009. Mineralogy and formation conditions of ores in the Bereznyakovskoe ore field, the Southern Urals, Russia. *Geol. Ore Deposits* 51 (5), 371–397.
- Savva, N.E., Pal'yanova, G.A., 2007. Genesis of gold and silver sulfides at the Ulakhan deposit (northeastern Russia). *Russian Geology and Geophysics (Geologiya i Geofizika)* 48 (10), 799–810 (1028–1042).
- Savva, N.E., Pal'yanova, G.A., Kolova, E.E., 2010. Gold and silver minerals in zone of secondary sulfide enrichment (Krutoe ore occurrence, northeastern Russia). *Vestnik SVNTs DVO RAN*, No. 1, 33–45.
- Savva, N.E., Pal'yanova, G.A., Byankin, M.A., 2012. The problem of genesis of gold and silver sulfides and selenides in the Kupol deposit (Chukotka, Russia). *Russian Geology and Geophysics (Geologiya i Geofizika)* 53 (5), 457–466 (597–609).
- Savva, N.E., Palyanova, G.A., Kolova, E.E., 2014. Gold and silver minerals and conditions of their formation at the Dorozhnoye deposit (Magadan region, Russia). *Nat. Resour.* 5, 478–495.
- Scott, S.D., Barnes, H.L., 1971. Sphalerite geothermometry and geobarometry. *Econ. Geol.* 66 (4) 653–669.
- Simon, G., Essene, E.J., 1996. Phase relations among selenides, sulfides, tellurides, and oxides: I. Thermodynamic properties and calculated equilibria. *Econ. Geol.* 91 (7), 1183–1208.
- Tagirov, B.R., Baranova, N.N., Zotov, A.V., Schott, J., Bannykh, L.N., 2006. Experimental determination of the stabilities of $Au_2S_{(cr)}$ at 25 °C and $Au(HS)_2^-$ at 25–250 °C. *Geochim. Cosmochim. Acta* 70 (14), 3689–3701.
- Tauson, V.L., Kravtsova, R.G., Lipko, S.V., Makshakov, A.S., Arsen'tev, K.Yu., 2018. Surface typochemism of native gold. *Dokl. Earth Sci.* 480 (1), 624–630.
- Volkov, A.V., Goncharov, V.I., Sidorov, A.A., 2006. *Gold and Silver Deposits of Chukchi Peninsula* [in Russian]. IGEM RA, Moscow.
- Voronin, M.V., Osadchii, E.G., Brichkina, E.A., 2017. Thermochemical properties of silver tellurides including empressite ($AgTe$) and phase diagrams for Ag–Te and Ag–Te–O. *Phys. Chem. Miner.* 44 (9), 639–653.
- Warmada, W., Lehmann, B., Simandjuntak, M., 2003. Polymetallic sulfides and sulfosalts of the Pongkor epithermal gold–silver deposit, West Java, Indonesia. *Can. Mineral.* 41, 185–200.
- Yokokawa, H., 1988. Tables of thermodynamic properties of inorganic compounds. *J. Natl. Chem. Lab. Ind.* 83, 27–118.
- Zharikov, V.A., Rusinov, V.L., 1998. *Metasomatism and Metasomatic Rocks* [in Russian]. Nauchnyi Mir, Moscow.
- Zhuravkova, T.V., Palyanova, G.A., Kravtsova, R.G., 2015. Physicochemical formation conditions of silver sulfoselenides at the Rogovik deposit, Northeastern Russia. *Geol. Ore Deposits* 57 (4), 313–330.
- Zhuravkova, T.V., Palyanova, G.A., Chudnenko, K.V., Kravtsova, R.G., Prokopyev, I.R., Makshakov, A.S., Borisenko, A.S., 2017. Physicochemical models of formation of gold–silver mineralization at the Rogovik deposit (Northeastern Russia). *Ore Geol. Rev.* 91, 1–20.